πNN system with two-term potentials in the P_{33} and P_{11} πN channels

C. Fayard and G. H. Lamot
Institut de Physique Nucléaire de Lyon, Institut National de Physique Nucléaire et de Physique des Particules–Centre National de la Recherche Scientifique, Université Claude Bernard, F-69622 Villeurbanne CEDEX, France

T. Mizutani
Department of Physics, Virginia Polytechnic Institute and State University, Blacksburg, Virginia 24061

B. Saghai
Service de Physique Nucléaire, Centre d'Etudes Nucléaires de Saclay, F-91191 Gif-sur-Yvette CEDEX, France
(Received 31 October 1991)

The πNN system is studied with two-term potentials for the πN interaction in the P_{33} and P_{11} channels. Such model systematics as the difference in the dominant πN P_{33} input, the effect of the so-called backward propagating pion, the choice of the relative momenta (magic vectors) at the isobar vertices, etc., are investigated. The results in the πd-πd, πd-NN, and NN-NN reactions at intermediate energies are compared with the available experimental data. The overall quality of the predictions by the present approach is roughly comparable to that based upon the one-term P_{33} isobar model supplemented by an appropriate *ad hoc* off-shell modification, but with a significant improvement in the description of the πd-NN asymmetry A_{y0}.

PACS number(s): 25.10.+s, 25.80.−e, 13.75.Gx

I. INTRODUCTION

During the past years, a number of experiments were conducted to obtain accurate data in the $\pi d \rightarrow \pi d$, $\pi d \leftrightarrow NN$, and $NN \rightarrow NN$ reactions at intermediate energies. In particular, high quality measurements of various polarization observables in the first two channels invited several theoretical investigations in these reactions.

The developments of the theoretical models leading to a unified description of the above processes were recently reviewed by Garcilazo and Mizutani [1]. We just recall the main aspects relevant to our present work. The first attempt to take into account the coupling to the NN channel (and thus the true pion absorption effect) in the πd problem was made by Afnan and Thomas [2]. Within the context of a pure three-body model, the pion absorption was simulated by assuming a πN-P_{11} bound state (denoted as N') with binding energy equal to the pion mass. This so-called bound-state picture (BSP) suffers from an essential difficulty due to the fact that N' behaves differently from the normal nucleon N when they form a two-nucleon system. As a consequence, (i) the effect of the pion absorption by *any* one of the two nucleons and its reemission by the other one cannot be included, (ii) the BSP gives hence only one of the two possible time orderings in the one pion exchange NN interaction, and (iii) the Pauli principle is violated in the NN sector (simulated by NN').

In the early eighties, a great effort was made to develop a coherent formulation where the three-body (πNN) and two-body (NN) channels are consistently coupled, thus free of the drawbacks encountered in BSP. Starting from different techniques, Avishai-Mizutani [3], Afnan-Blankleider [4], and Rinat *et al.* [5] have derived a similar set of equations for the coupled πNN-NN systems. This coupled πNN-NN approach (denoted as PNNA in [1]) takes into account the fact that the pion can be absorbed/emitted by *either* one of the two nucleons. Moreover, with a proper self-energy dressing of the NN propagator and the dressing of the πNN vertices when the nonpole contribution to the πN P_{11} channel is included, the PNNA equations satisfy two and three particle unitarity (see Refs. [3, 4]). So, the PNNA model describes in an unified manner the $\pi d \rightarrow \pi d$, $\pi d \leftrightarrow NN$, and $NN \rightarrow NN$ reactions as well as those with three-body (πNN) final states. We shall call these reaction channels collectively *the πNN system.*

In our previous work [6] (hereafter refered to as LY87), we have presented extensive calculations exploiting the PNNA approach at intermediate energies. There, the equations adopted were relativistic, compatible with two and three body unitarity, and the basic two-body inputs were the NN $^3S_1$-$^3D_1$ and all the πN S and P partial waves parametrized as rank-1 separable interactions, except for the P_{11} πN channel which received a special treatment as discussed later. All these two-body contributions were taken into account to all orders in iterations in the context of three-body scattering theories.

Two most important ingredients are the P_{33} and P_{11} πN channels, the former in particular. In LY87, we have made the usual assumption of the Δ-isobar dominance where the interaction of this partial wave was represented by a one-term separable potential. The parameters of

the potential were the bare Δ mass, the $\pi N\Delta$ coupling constant, and the cutoff momentum Λ for the $\pi N\Delta$ vertex. These parameters were determined by fit to the P_{33} phase shift. It has been well established by now that in this type of models the value of the cutoff mass Λ at the $\pi N\Delta$ vertex deduced from the fit cannot be very different from ~ 300 MeV/c assuming a monopole form factor. The fit to the phase shift up to about $T_\pi^{\rm lab} = 400$ MeV is so good by this type of model, one would least doubt its validity. But once this P_{33} model was used in the πNN equations [6], one found that it leads to a serious underestimation of the effect of pion production in the πd-NN and NN-NN reactions. The source of this trouble was soon recognized as the off-shell behavior of this $\pi N\Delta$ vertex which cuts too strongly the medium to high momentum transfer from the pion. Note that the only process that escaped this trap was the elastic pion-deuteron channel, the major contribution to which involves only a small amount of momentum transfer and the P_{33} input stays almost on-shell.

In order to implement an appropriate off-shell structure in the P_{33} channel, we applied *off-shell modifications* as described in LY87. Essentially, this was to introduce a new vertex with a larger value of the cutoff mass while conserving unitarity. A similar prescription was also adopted in the P_{11} channel. The corresponding off-shell parameters were determined by obtaining the correct magnitude of the πd-NN differential cross sections at $T_\pi^{\rm lab} = 142$ MeV. Differing in minor details, essentially the same strategy has been adopted by Lee and Matsuyama [7], and by Garcilazo [8]. We briefly summarize the merits and demerits of the LY87 results below.

(i) The overall description of the πd elastic scattering observables is rather satisfactory. However, the model fails to reproduce the T_{20} polarization at backward angles, and to a less extent the large angle differential cross section for $T_\pi^{\rm lab} > 180$ MeV. We have recently improved this situation, particularly above the delta resonance energy, by including the contribution which we called the Jennings mechanism [9].

(ii) In the πd-NN sector, the differential cross section is well explained by the model at $T_\pi^{\rm lab} = 142$ and 180 MeV, but is underestimated at 256 MeV, and its curvature is not really well reproduced. Concerning the asymmetry A_{y0}, the pronounced dip observed experimentally around $\theta_{\rm c.m.} = 90^0$ is not reproduced. Besides, the overall magnitude becomes too large with increasing energy.

(iii) In the elastic NN channel, the phase shifts in the dominant ${}^1D_2$ and ${}^3F_3$ partial waves are well reproduced up to $T_N^{\rm lab} \sim 1$ GeV, provided that the *heavy meson exchange* contributions are introduced to get enough repulsion at $T_N^{\rm lab} \geq 500$ MeV. The inelasticity $\eta({}^1D_2)$ is described well up to 700 MeV, but rapidly deviates above this energy from the result of the Virginia Polytechnic Institute (VPI) analysis [10]. The most serious deficiencies are the lack of inelasticity in the ${}^3F_3$ partial wave and the poor description of the ${}^1S_0$ and ${}^3P_1$ phase shifts. The peripheral partial waves for isospin 0 and 1 NN channels are well reproduced up to 1 GeV.

Summing up, in conventional meson-baryon approaches to the πNN system, one is quite aware that the key inputs are the πN P_{33} and P_{11} channels. In particular, one now knows that the simple isobar model for P_{33} with a very soft cutoff cannot give enough pion production strength. As stated above, we introduced an *ad hoc off-shell modification* in these channels to obtain an adequate description of the reactions in this system. Is there any alternative picture to meet our goal?

Recently, Tanabe and Ohta [11, 12] proposed another and, in our opinion, more satisfactory approach (hereafter refered to as the TO model) based on a *two-potential model* to describe the P_{33} partial wave. Their approach is quite similar to the one used in our model for the P_{11} channel [13]. The potential is written as a sum of two parts, the resonant and background interactions. Each part is parametrized in a separable form, and the cutoff parameter of the resonant interaction is chosen to be compatible with the values used, e.g. in Ref. [7]. This two-term picture is more in line with the underlying quark picture: the P_{33} amplitude receives contributions from (i) the *elementary* Δ which has no decay width, (ii) the crossed nucleon pole term, and (iii) the iterates thereof. The P_{11} interaction employed by TO is also of the two-term form, as discussed in the next section. It should be noted that (i) the TO calculations are based on the BSP approach (as explicitely stated in Ref. [11]), (ii) the contribution of the *backward propagating pion* is taken into account in the πNN three-body propagator, and (iii) the P_{11} partial wave is treated as a single entity in the πNN equations (i.e., the pole and nonpole parts are not separated).

The first calculations of Tanabe and Ohta included only the P_{33} and P_{11} partial waves, thus were limited to the NN-NN sector. As may be found in Ref. [11], the ${}^1D_2$ phase shift (real part) is well reproduced, but the inelasticity parameter is underestimated for $T_N^{\rm lab} \leq 700$ MeV, while in the ${}^3F_3$ channel the phase shift is too much attractive and the inelasticity is underestimated. Furthermore, phase shifts for other nonperipheric partial waves are poor. This should be due to the fact that no heavy meson exchanges were considered in their model.

An extended version of this model [12] included all the S, P and the ${}^3D_1$ NN partial waves (in the presence of the pion spectator), as well as the *small* πN partial waves (i.e., S_{11}, S_{31}, P_{13}, and P_{31}). So, it was possible to obtain the πd-NN observables. However, the elastic πd sector was not investigated.

By examining the results of Ref. [12], one may draw the following conclusions concerning the *full* TO model.

(i) In the NN sector, the only significant improvement resulting from the *full* calculation is an increase in the ${}^1D_2$ inelasticity below $T_N^{\rm lab} = 700$ MeV, leading to a nice agreement with the data. This is due primarily to the inclusion of the coupling to the πd channel as clarified by our previous work [14].

(ii) In the πd-NN sector, the differential cross sections are in reasonable agreement with the data. As shown by Tanabe and Ohta, the backward propagating pion contribution is indispensable for obtaining the cor-

rect magnitude for these cross sections. However, the TO model tends to give the wrong curvature which gets worse with increasing energy. As for the asymmetry A_{y0}, the prediction does not agree with the data, except at very forward and backward angles. The overall magnitude is too large at all energies, especially at $T_\pi^{\rm lab} = 80$ MeV where the theoretical curve shows a broad maximum around $\theta_{\rm c.m.} = 90^0$, contrary to the deep minimum in the data. At higher energy, a minimum appears whose detailed structure depends upon models adopted for the P_{11} and P_{33}, but the curves still remain too high.

The motivation for the present article comes from the Tanabe-Ohta model and its consequences summarized above. We would like to further look into this model regarding the following points.

(i) TO have not studied the elastic pion-deuteron sector. This should be investigated to complete the predictions in various two-body channels of the πNN system.

(ii) Since two-term models for the P_{33} interaction appear to be more realistic than the single term interaction and may completely replace the latter in the near future (in fact, an application to the photopion production on the nucleon exists [15]), we want to study their off-shell nature. For this purpose we have introduced an interaction whose analytic expression is quite different from the TO P_{33} interactions.

(iii) The TO treatment of the P_{11} interaction in the πNN equation is not the same as ours (concerning its explicit decomposition and the application of the Pauli principle). We thus combine the TO P_{33} and our P_{11} interactions together with the *pole + nonpole* decomposition of the latter in the way adopted in LY87. As will be discussed later, this *mixed* model is found to give an improved description in certain observables, particularly in the asymmetry parameter in the πd-NN reaction at intermediate energies, which was impossible to obtain with usual three-body models.

Our present work is thus an extension of the LY87 calculations, devoted to studying detailed systematics centering around two-term P_{33} interactions (in particular the TO model and its variation/extension) and the backward pion effect. We believe that this type of investigation, although rather technical, is indispensable in view of the fact that (a) theoretical study of the πNN system has now reached the point where qualitative agreement with data is no longer sufficient, and (b) that the πNN system will soon be studied extensively by electromagnetic probes, where reliable models for the strong interaction sector are called for.

The organization of this article is as follows. Sec. II summarizes the theoretical aspects of the model investigated. In Sec. III, we give a series of results obtained with the original TO model inputs for the NN-NN, πd-NN, and πd-πd reactions, and, after a comparison with the LY87 model, we present our calculations with the *mixed* model. Finally, our conclusions are drawn in Sec. IV.

II. MODEL ASPECTS

Although the main idea of what is discussed below could be found in the existing literature, we present it for the sake of clarity and to be self-contained.

A. Two-potential model for the P_{33}

In the Tanabe-Ohta model [11,12], the πN P_{33} channel is considered as a superposition of two open channels, the πN continuum and the Δ-isobar state: the *background* and *resonant* contributions, respectively. The t matrix is assumed to satisfy the usual scattering equation:

$$t(s) = V + VG_0(s)t(s), \tag{1}$$

where G_0(s) is the πN free propagator and the driving potential V is the sum of two terms:

$$V = v_B + v_R. \tag{2}$$

v_R is the resonant interaction parametrized as

$$v_R = |g_1\rangle\lambda_1\langle g_1|, \quad \lambda_1 = \frac{2m_0}{s - m_0^2}\ , \tag{3}$$

where m_0 is the bare-Δ mass and s the πN total c.m. energy squared. v_B is the background interaction which is absent in the conventional Δ-isobar model (i.e. one term separable model). The physical origin of this term can be attributed to the crossed nucleon pole process and is treated as a purely phenomenological separable potential:

$$v_B = |g_2\rangle\lambda_2\langle g_2|, \quad \lambda_2 = -\frac{1}{m_\pi}. \tag{4}$$

The t matrix is easily obtained as

$$t(s) = \sum_{i,j=1}^{2} |g_i\rangle\tau_{ij}(s)\langle g_j|\ . \tag{5}$$

The quantities τ_{ij} are the elements of a 2×2 matrix:

$$[\tau^{-1}(s)]_{ij} = \lambda_i^{-1}\delta_{ij} - \sigma_{ij}(s)\ , \tag{6}$$

where σ_{ij} is the overlap integral of the form factors:

$$\sigma_{ij}(s) = \langle g_i|G_0(s)|g_j\rangle \tag{7}$$

which are chosen as

$$g_i(p) = p\,(p^2 + \Lambda_i^2)^{-n}. \tag{8}$$

Two parametrizations have been determined, corresponding respectively to dipole ($n = 2$, model-A) and monopole ($n = 1$, model-B) form factors. The parameters are fitted to the experimental P_{33} phase shifts. The obtained values may be found in Table I of Ref. [11]. In practice, the cutoff parameter Λ of the resonant part was chosen by Tanabe and Ohta to be 1000 MeV/c for model A and 1200 MeV/c for model B. The first choice corresponds to $\Lambda/\sqrt{2} \sim 700$ MeV/c for a monopole form factor, in line with the values used in Ref. [7]. The second choice simulates the value used in the peripheral

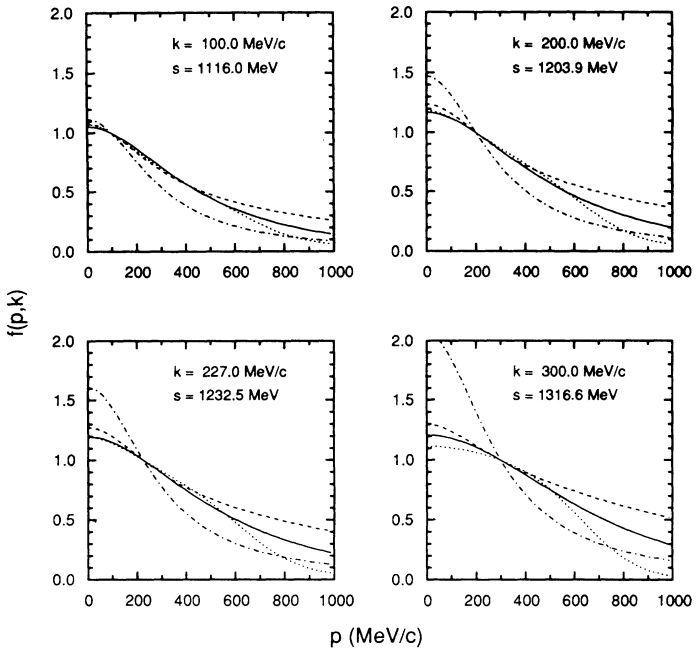

FIG. 1. Half-off-shell amplitudes $f(p,k)$ of the P_{33} partial wave at fixed on-shell momenta k ($\sqrt{s}$ is the total energy). Curves are two-potential model A (solid line) and model B (dashed line) from Tanabe and Ohta, and Saxon (dotted line). The dash-dotted curves correspond to the (one term) Δ-isobar model used in LY87.

models for pion production; see, for example, Ref. [16]. Note that the bare-Δ mass is $m_0 = 1740$ MeV for model B, which requires a huge mass renormalization ($\sim$ 500 MeV), while model A has a more reasonable value ($m_0 =$ 1410 MeV).

The πN P_{33} phase shift predicted by models A and B, and also by the Δ-isobar model, cannot be distinguished from the experimental data (see Fig. 2 in Ref. [11]), indicating that all the models are, to a high accuracy, on-shell equivalent. However, the off-shell behavior of the t matrices are different. This can be seen by considering the half-off-shell amplitude $f(p,k)$ defined as

$$f(p,k) = \frac{k}{p}\frac{R(p,k)}{R(k,k)}, \tag{9}$$

where k is the on-shell momentum, and $R(p,k)$ is the half-off-shell reaction matrix. As shown in Fig. 1, the two models A and B have globally the same type of behavior; in particular the slopes are quite similar near the on-shell point ($p \sim k$), while the (one term) Δ-isobar model gives a much faster damping, especially at high energies. One may expect that such differences will be reflected in the three-body sector.

To further study the consequences of the different off-shell behaviors, we have constructed another two-term potential where the form factor of the resonant part is completely different from the usual monopole or dipole forms, namely, of a Saxon-Woods type:

$$g_1(p) = S_R\, p \left[1 + \exp\left(\frac{p^2 - p_0^2}{\beta_R^2}\right)\right]^{-1}. \tag{10}$$

A monopole form is chosen for the background part:

$$g_2(p) = S_B\, p\,(p^2 + \Lambda_B^2)^{-1}. \tag{11}$$

The corresponding strengths are $\lambda_1 = 1/(s - m_0^2)$ and $\lambda_2 = -1$. The fitted parameters are given in Table I. The resulting half-off-shell amplitude shown in Fig. 1 is quite similar to model A, except at high p values ($p \geq 600$ MeV/c) where the Saxon form factor gives a stronger damping.

The characteristic of these two-potential models is that the half-off-shell amplitude $f(p,k)$ is a rather smooth function of p and k compared with the Δ-isobar model. One then naturally expects that the two-potential mod-

TABLE I. Parameters of the two-potential model for the P_{33} channel defined in Eqs. (10) and (11). The index R refers to the Saxon resonant part (S_R is dimensionless), and B to the monopole background part.

S_R	β_R (fm^{-1})	p_0 (fm^{-1})	m_0 (MeV)	S_B (fm^{-1})	Λ_B (fm^{-1})
63.02	2.15	2.86	1351.4	46.38	1.48

els may give quite different consequences in the πNN system as compared with the one-term isobar model.

B. Two-potential model for the P_{11}

In the TO approach, the P_{11} channel is treated in the same way as the P_{33} with the following modifications.

(i) The parameters search was done with the two constraints that the t matrix has a pole at the nucleon mass ($\sqrt{s} = m_N$) and that the bare coupling constant f is renormalized at that pole to the value $f^2/4\pi = 0.08$.

(ii) In order to take into account the large effects of inelasticity which develop for $T_N^{\rm lab} \geq 150$ MeV, the $\sigma_{ij}(s)$ integral is evaluated with the modified πN propagator:

$$\widetilde{G}_0(p;s) = G_0(p;s)/\hat{\eta}(p), \tag{12}$$

where $\hat{\eta}$ is a parametrization of the experimental inelasticity.

(iii) The effect of the Roper resonance is introduced by defining the strength of the background part in an energy-dependent way:

$$\lambda_2(s) = -\frac{c}{m_\pi} + \frac{2m_R}{s - m_R^2}, \tag{13}$$

where c is an adjustable parameter and m_R must be varied around the Roper mass.

Two vertex models A (dipole) and B (monopole) are considered, corresponding to those used in the P_{33} case. Assuming that the nucleon and Δ have a similar spatial extension, the P_{11} cutoff momentum of the resonant part is chosen identical to the P_{33} one, and the remaining free parameters are fitted to the P_{11} phase parameters (see Table II in Ref. [11]).

In our LY87 approach, the P_{11} channel has been parametrized according to the method of Mizutani *et al.* [13]. The total t matrix is written as the sum of a pole (repulsive) and nonpole (attractive) part, namely, $t = t_P + t_{NP}$. The nonpole part is assumed as rank-1 separable:

$$t_{NP}(p,p';s) = g(p)R_{NP}(s)g(p'). \tag{14}$$

After dressing the πNN vertex by virtual pions as required by two-body unitarity, the pole part reads

$$t_P(p,p';s) = h(p;s)R_N(s)h(p';s), \tag{15}$$

where h is the dressed πNN vertex (expressed in terms of the bare πNN vertex and of t_{NP}), and R_N the dressed nucleon propagator (evaluated in terms of h). The parameters were fitted to the data.

The most important difference between our LY87 description of the P_{11} channel and that of Tanabe and Ohta is that in the former the pole and nonpole parts of the total t matrix appear separately in the πNN equation, while in the TO model the P_{11} t matrix appears as a single entity. The consequence is that once imbedded in the πNN system, the TO model retains the Pauli forbidden NN states. Its effect as compared with the results of the correct treatment is discussed semiquantitatively in Ref. [11].

C. Other two-body inputs

When the two-body inputs are limited to the P_{33} and P_{11} πN channels, the solution to the πNN-NN equations can give only amplitudes for the NN elastic scattering, and eventually for the $NN \to N\Delta$ and $NN \to \pi NN$ reactions. In order to obtain also the amplitudes for the πd-πd and πd-NN channels, one obviously must add the NN $^3S_1$-$^3D_1$ partial wave (in the presence of the spectator pion): the d channel. We want to remind the reader the importance of the effect of coupling to the πd channel on intermediate energy NN scattering [14], at least in the $^1D_2$ and $^3F_3$ partial waves up to $T_N^{\rm lab} \sim 700$ MeV (this has been confirmed in Refs. [11, 12]). Moreover, an adequate description of the differential cross sections and polarization observables of the πd-πd and πd-NN reactions can be obtained only if the *small* S and P πN partial waves (i.e., S_{11}, S_{31}, P_{13} and P_{31}) are also included. Finally, the extra S and P NN partial waves (i.e., $^1S_0$, $^1P_1$ and $^3P_{0,1,2}$) have a non-negligible effect on the πd-NN observables, as noticed in the previous calculations [17, 18].

The small πN partial waves are parametrized by Tanabe and Ohta as relativistic rank-1 separable potentials. The parameters are fitted to the observed phase shifts up to $T_\pi^{\rm lab} \sim 400$ MeV, as described in Ref. [12]. In these channels, we have used the same parametrizations as in our previous studies, namely, the relativistic rank-1 potentials of Schwarz *et al.* [19]. As we will see later, these two sets of parametrizations do not bring significant changes in the πNN observables.

For the NN interaction, TO have retained the d (viz., $^3S_1$-$^3D_1$), $^1S_0$ and all P partial waves. They chose the nonrelativistic separable parametrizations of the Paris potential proposed by Haidenbauer and Plessas (HP, Ref. [20]), and relativized them by using the minimal relativity prescription. The HP potentials, which are constructed following the Ernst-Shakin-Thaler method, give a realistic representation of the on-shell as well as off-shell properties of the Paris potential. The rank of the parametrization depends upon the partial wave: rank 4 for $^3S_1$-$^3D_1$ (or rank 1 in a simplified version), rank 1 for $^1S_0$, rank 2 for $^1P_1$ and $^3P_{0,1}$, and rank 3 for $^3P_2$-$^3F_2$ (note that for this last channel, Tanabe and Ohta did not specify what parameters they have used, since apparently only the $^3P_2$ part of this coupled channel was retained in their calculation). We remark that the form factors of the HP potentials are written as a sum of four rational functions. Therefore, such interactions require a considerable increase in the memory size and computing time in the numerical solution of the three-body equations. For this reason, in the NN $^3S_1$-$^3D_1$ channel we have adopted our own relativistic interaction of rank 1 already defined in LY87, and the contributions of the extra NN partial waves have been ignored.

D. Three-body equations

The basic PNNA equations for the coupled πNN-NN sytems are now well known. With separable interactions for the πN and NN two-body subsystems, the equations for the $NN \to \pi d$ and $NN \to NN$ reactions read schematically (see, for example, Ref. [3]):

$$\begin{bmatrix} X_{dN} \\ X_{\Delta N} \\ X_{NN} \end{bmatrix} = \begin{bmatrix} Z_{dN} \\ Z_{\Delta N} \\ Z_{NN} \end{bmatrix} + \begin{bmatrix} 0 & Z_{d\Delta} & Z_{dN} \\ Z_{\Delta d} & Z_{\Delta\Delta} & Z_{\Delta N} \\ Z_{Nd} & Z_{N\Delta} & Z_{NN} \end{bmatrix} \times \begin{bmatrix} R_d & 0 & 0 \\ 0 & R_\Delta & 0 \\ 0 & 0 & R_N \end{bmatrix} \begin{bmatrix} X_{dN} \\ X_{\Delta N} \\ X_{NN} \end{bmatrix} . \tag{16}$$

In the above equation, X are the three-body amplitudes, Z the Born terms (or driving terms), and R the two-body propagators in three-body Hilbert space. The lower indices refer to the various three-body channels, each of them being denoted by the name of its interacting pair, as usual: the index N refers to the πN-P_{11} pole part, Δ to all the other πN isobars (including the P_{33} channel and the P_{11} nonpole part), and d to all NN isobars. As pointed out in the Introduction, both time orderings are included in the OPE amplitude Z_{NN} (since the pion can be absorbed and emitted by either one of the two nucleons), and R_N is the dressed two nucleon propagator.

The $\pi d \to \pi d$ and $\pi d \to NN$ reactions are obtained through a similar set of equations with the same kernel $[Z][R]$, only the second lower index N in the column matrices X and Z must be replaced by d (with $Z_{dd} \equiv 0$). The X_{dd}, X_{Nd}, and X_{NN} amplitudes evaluated on-shell correspond to the physical amplitudes for the $\pi d \to \pi d$, $\pi d \to NN$, and $NN \to NN$ reactions, respectively (here, d stands for the deuteron channel).

In what has been written above, the explicit decomposition of the the total t matrix of the P_{11} partial wave into pole and nonpole parts is assumed [recall Eqs. (14) and (15)], so that the corresponding three-body channels appear separately in the equations. As a consequence, the Pauli principle will take place only in the intermediate NN channels coming from the pole part. We also note that the X, Z and R terms must be understood as matrices when two-body parametrizations of rank > 1 are used. For instance, if a two-potential model is chosen for the $\Delta(P_{33})$ πN channel, the corresponding propagator R_Δ is a 2×2 matrix [the elements of which are the τ_{ij} defined in Eq. (6)], $X_{\Delta N}$ is a 2×1 matrix, and so on.

Upon adopting the two-potential model of Tanabe and Ohta for the P_{11} channel, the following modifications are in order. Since this channel is treated as a single entity in the three-body equations, the Δ index now refers to all πN isobars but the P_{11}, and N refers to the whole P_{11}. As we just explained for the case of the P_{33}, the R_N propagator is then a 2×2 matrix, X_{Nd} a 2×1 matrix, X_{NN} a 2×2 matrix, etc. The physical $NN \to NN$ amplitude $\widetilde{X}_{NN}$ is related to the matrix elements of X_{NN} (evaluated on-shell) through

$$\widetilde{X}_{NN} = \sum_{n,m=1,2} Z_n \, X^{nm}_{NN} \, Z_m . \tag{17}$$

Here, the indices n, m run over the values 1 and 2 which correspond, respectively, to the pole and nonpole parts of the P_{11} interaction, according to the notations used in Secs. II A and II B. The coefficients Z_1 and Z_2 are related to the renormalization constant of the nucleon wave function, as defined in Eq. (2.25) of Ref. [11]. The physical amplitude for the $\pi d \to NN$ reaction is defined likewise in terms of the matrix elements of X_{Nd}:

$$\widetilde{X}_{Nd} = \sum_{n=1,2} Z_n \, X^{n}_{Nd} . \tag{18}$$

E. Magic vectors

The driving terms Z in Eq. (16) are effective potentials for the exchange of one particle between two isobars. Let us consider the process depicted in Fig. 2 where particle k is exchanged between isobars b and a formed from particles k and i, and j and k, respectively:

$$j + b(= k + i) \to i + a(= j + k).$$

The corresponding driving term Z_{ab} has the following expression:

$$\langle \mathbf{q} | Z^{nm}_{ab}(s) | \mathbf{q}' \rangle = g^{(n)}_a(\mathbf{p}_a) \, G^{(3)}(\mathbf{q}, \mathbf{q}'; s) \, g^{(m)}_b(\mathbf{p}_b) . \tag{19}$$

Here, g's are the vertex form factors for *two particles* $\leftrightarrow$ *isobar*, with $n = 1, ..., n_a$ and $m = 1, ..., m_b$, where n_a and m_b are the ranks of the potentials used to describe the a and b two-body subsytems, respectively. The vectors $\mathbf{q}$ and $\mathbf{q}'$ are the momenta of the spectator particles i and j, $\mathbf{p}_a$ and $\mathbf{p}_b$ are the *magic vectors* at the vertices a and b, and s is the total energy squared. The free three-body propagator is written in our relativistic approach as

$$G^{(3)}(\mathbf{q}, \mathbf{q}'; s) = \frac{E_{\mathbf{q}} + E_{\mathbf{q}'} + E_{\mathbf{q}+\mathbf{q}'}}{E_{\mathbf{q}+\mathbf{q}'}[s - (E_{\mathbf{q}} + E_{\mathbf{q}'} + E_{\mathbf{q}+\mathbf{q}'})^2 + i\epsilon]} , \tag{20}$$

where $E_{\mathbf{q}}$, $E_{\mathbf{q}'}$, and $E_{\mathbf{q}+\mathbf{q}'}$ are the relativistic energies of particles i, j, and of the exchanged particle k, respectively:

$$E_{\mathbf{q}} = \sqrt{\mathbf{q}^2 + m_i^2} \quad , \quad E_{\mathbf{q}'} = \sqrt{\mathbf{q}'^2 + m_j^2}$$
$$E_{\mathbf{q}+\mathbf{q}'} = \sqrt{(\mathbf{q} + \mathbf{q}')^2 + m_k^2} . \tag{21}$$

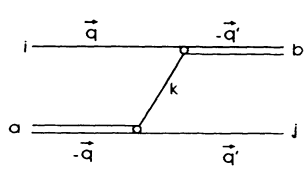

FIG. 2. The Z_{ab} Born term corresponding to the exchange process of particle k between the two isobars b $(= k + i)$ and a $(= j + k)$.

The magic vectors $\mathbf{p}_a$ and $\mathbf{p}_b$ are an extension to the relativistic domain of the ordinary relative momenta at the vertices used in the nonrelativistic approach. According to the work of Aaron, Amado, and Young [21], they are constructed in such a way that their modulus and scalar product are Lorentz invariant. As pointed out by Rinat and Thomas [22], the magic vectors are written as linear combinations of $\mathbf{q}$ and $\mathbf{q}'$:

$$\begin{aligned}\mathbf{p}_a &= \mathbf{q}' + \rho(q,q';x)\mathbf{q}, \\ \mathbf{p}_b &= -\mathbf{q} - \rho(q',q;x)\mathbf{q}',\end{aligned} \tag{22}$$

where $x = \hat{\mathbf{q}}\cdot\hat{\mathbf{q}}'$. The expression of the ρ function depends on whether the exchanged particle is put on its mass shell (*case a*) or not (*case b*).

In *case a* we have

$$\rho(q,q';x) = \xi_{\mathbf{q}}^{-1/2}[E_{\mathbf{q}'} + \mathbf{q}\cdot\mathbf{q}'(\xi_{\mathbf{q}}^{1/2} + E_{\mathbf{q}'} + E_{\mathbf{q}+\mathbf{q}'})^{-1}] \tag{23}$$

with

$$\xi_{\mathbf{q}} = (E_{\mathbf{q}'} + E_{\mathbf{q}+\mathbf{q}'})^2 - \mathbf{q}^2. \tag{24}$$

This prescription was used in all our previous calculations.

In *case b*, which corresponds to the spectator particle put on its mass shell, the ρ function reads

$$\rho(q,q';x) = \sigma_{\mathbf{q}}^{-1/2}[E_{\mathbf{q}'} + \mathbf{q}\cdot\mathbf{q}'(\sigma_{\mathbf{q}}^{1/2} + s^{1/2} - E_{\mathbf{q}})^{-1}], \tag{25}$$

where $\sigma_{\mathbf{q}}$ is the squared invariant mass of isobar a:

$$\sigma_{\mathbf{q}} = (\sqrt{s} - E_{\mathbf{q}})^2 - \mathbf{q}^2 = s - 2\sqrt{s}\,E_{\mathbf{q}} + m_i^2. \tag{26}$$

This choice is retained in the work of Garcilazo [8], and also in the Tanabe-Ohta calculations. From Eq. (25), it is clear that the *case-b* magic vectors cannot be defined where $\sigma_{\mathbf{q}} = 0$ or $\sigma_{\mathbf{q}'} = 0$. This situation occurs when the driving term Z_{ab} is put in the three-body integral equation. In order to avoid the violation of unitarity, the integral must be cut off at q_c where $\sigma_{q_c} = 0$. From Eq. (26), we have

$$q_c = (s - m_{\text{spec}}^2)/2\sqrt{s}, \tag{27}$$

where m_{spec} is the mass of the spectator particle. Since only the pion and the nucleon can be spectators in the various Born terms involved in Eq. (16), we must take as q_c the smallest value, namely that corresponding to a spectator nucleon. In principle, the method of contour rotation in its original form used to bypass the three-body branch cuts can no longer be applied because the integral is cut off at a finite value, unless the angle of rotation is chosen sufficiently small, as explained in Ref. [11].

The ambiguity in the definition of the magic vectors is inherent to the relativistic three-body model reduced to retain only three-dimensional integrations, and there is no *a priori* argument to make a unique choice. As stated above we prefer *case a* which does not suffer from the numerical difficulties encountered with *case b*.

F. Backward propagating pion

In a nonrelativistic three-body approach to the πNN system and in its straightforward relativistic extension like Refs. [3,6], the Δ isobar (i.e., any πN isobar, except the P_{11} pole part) can only emit the pion, but cannot absorb it: for example, the graph shown in Fig. 3 for the $NN \leftrightarrow N\Delta$ amplitude is not included (this is also the case for the $N\Delta \rightarrow N\Delta$ amplitude). This effect is often called the *backward propagating pion contribution* which is naturally included in a covariant (Feynman) approach. Lacking this contribution results in underestimating the pion exchange driving term, for example the NN-$N\Delta$ transition potential, by a factor of two in the static limit as compared with the same potential from one boson exchange (OBE) models. See, for example, Refs. [1, 23, 24].

In order to simulate this contribution within the BSP model, Tanabe and Ohta have modified the expression of the πNN three-body propagator entering in the $NN' \rightarrow NN'$, $NN' \leftrightarrow N\Delta$, and $N\Delta \rightarrow N\Delta$ amplitudes. Namely, following the prescription of Kloet and Silbar [24], $G^{(3)}$ is written as the sum of the *forward (fw)* and *backward (bw)* propagators:

$$G^{(3)} = G_{fw}^{(3)} + G_{bw}^{(3)}. \tag{28}$$

$G_{fw}^{(3)}$ is the only piece retained in the usual calculations and is evaluated through Eqs. (20) and (21) with $m_i = m_j = m_N$, and $m_k = m_\pi$, and $G_{bw}^{(3)}$ is taken as one-half of the static pion propagator:

$$G_{bw}^{(3)} = -\frac{1}{2E_{\mathbf{q}+\mathbf{q}'}^2}. \tag{29}$$

This term does not violate unitarity and it ensures that the three-body propagator has the correct static limit.

In the present work based on the PNNA approach, we use the same prescription for the πNN propagator [Eqs. (28) and (29)] *only* in the $Z_{N\Delta}$, $Z_{\Delta N}$, and $Z_{\Delta\Delta}$ Born terms. This is denoted as the *backward pion contribution* throughout the next section. Notice that Z_{NN} contains already both time orderings as mentioned above, so the backward pion contribution must not be included in this term in order to avoid double counting.

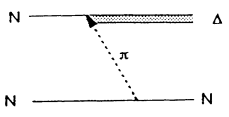

FIG. 3. Diagram corresponding to the backward propagating pion contribution to the $NN \leftrightarrow N\Delta$ amplitude. Δ is any πN isobar, except the P_{11} pole part.

III. RESULTS FOR THE πNN OBSERVABLES

In this section, we present our results for the differential cross sections and spin observables of the $\pi d \to \pi d$ and $\pi d \leftrightarrow NN$ reactions, and for the NN phase shift parameters. In the first subsection, the Tanabe-Ohta approach with a slightly different set of input in minor two-body channels is investigated. In the second subsection, this model is investigated in details in order to understand the origin of the differences with the LY87 model. We present in the third subsection a *mixed* model which combines the best aspects of these two models. We note that in the calculations presented below, the system of three-body coupled integral equations is numerically solved *exactly* using matrix inversion technique.

A. Results with the Tanabe-Ohta inputs

As a first step, we have modified our LY87 code in order to introduce the TO two-body input as well as the backward pion contribution to $Z_{N\Delta}$, $Z_{\Delta N}$, and $Z_{\Delta\Delta}$. We have confirmed that we can reproduce the results of Tanabe and Ohta for the $^1D_2$ and $^3F_3$ phase parameters, using the *simplified* version of Ref. [11] where only the P_{11} and P_{33} contributions are retained. Next, we have considered the *full* inputs of Ref. [12]. For the reasons given at the end of Sec. II C, we have limited the NN interaction to the d-channel contribution. For the πN P_{11} and P_{33} channels, we have chosen model B, since it gives better πd-NN cross sections than model A in the Tanabe-Ohta calculations [see Fig. 3(a) in Ref. [12]]. To be coherent with the TO calculations, *case-b* magic vectors were used, and only the P_{13} and P_{31} small πN channels were retained. Our results for the πd-NN reaction at $T_\pi^{\rm lab}$ = 142 MeV are shown in Fig. 4 (solid line). They are in reasonable agreement with those of Tanabe and Ohta shown in Figs. 3(a) and 3(b) of Ref. [12]: our differential cross section is $\sim$ 15% lower at $\cos^2\theta = 1$ and exhibits the same curvature, and our asymmetry parameter A_{y0}, which is very sensitive to the details of the model, has a lower ($\sim$ 20%) and more pronounced structure in the angular range $\theta_{\rm c.m.} \simeq 50^0 - 130^0$, in better agreement with the data. These differences should be attributed to the contributions of the nondominant NN channels, in accordance with our previous experience [17, 18].

Next, we have considered the πd elastic scattering which was not investigated in the work of Tanabe and Ohta. In Fig. 5 (solid line), we present our results for some selected observables at $T_\pi^{\rm lab}$ = 142 MeV in the same conditions as above. The theoretical curves reproduce fairly well the experimental data, except the vector polarization it_{11} which stays too small in all the angular range.

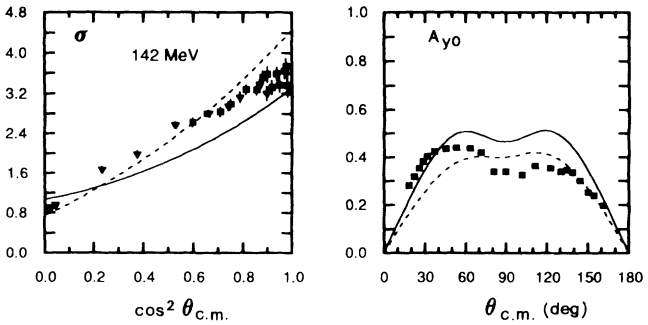

FIG. 4. πd-NN differential cross section σ (in mb/sr) and asymmetry parameter A_{y0}, calculated at $T_\pi^{\rm lab}$ = 142 MeV with the Tanabe-Ohta inputs (*case-b* magic vectors, backward pion). Model B is used for the P_{11} and P_{33} channels, and the d-NN and P_{13}, P_{31} πN partial waves are retained (solid line). The dashed line curves correspond to the MTO(b)-B model including all the small πN partial waves (see Table II). The data are from the references cited in LY87.

The above results are obtained *without* the πN S partial waves contributions. The reason invoked by TO to neglect these channels is that they bring an undesirable enhancement of the low energy πd-NN total cross sections (see Fig. 8 in Ref. [12]). Adding these contributions has in fact improved the πd-NN cross section at 142 MeV (Fig. 4, dashed line). However, the curvature of the differential cross section still remains incorrect, and the structure in the asymmetry A_{y0} is too soft compared with the experimental data. In the πd elastic sector, it_{11} is well reproduced when these contributions are included, while the other observables are practically unchanged (Fig. 5, dashed line). Similar conclusions hold at $T_\pi^{\rm lab}$ = 180 and 256 MeV. It is therefore preferable to include the contributions from *all* the small πN partial waves for studying the πNN system at intermediate energy. We should remark here that these curves are obtained with the parametrizations of the d-NN and small πN channels used in LY87, since we have found that using the original TO parametrizations in these channels leads to practically identical results. This model will be hereafter refered to as the *modified* Tanabe-Ohta model

TABLE II. Characteristics of the different models used in this paper. All these models have the d-NN and *small* πN from LY87.

Model	P_{33}	P_{11}	Backward pion	Magic vectors	Off-shell
MTO(a)-A,B	two-potential model (A, B)		yes	case a	no
MTO(b)-A,B	from Tanabe-Ohta		yes	case b	no
LY87	Δ-isobar	P+NP	no	case a	yes
LYTO	two-potential (models A, B, Saxon)	P+NP	yes	case a	no

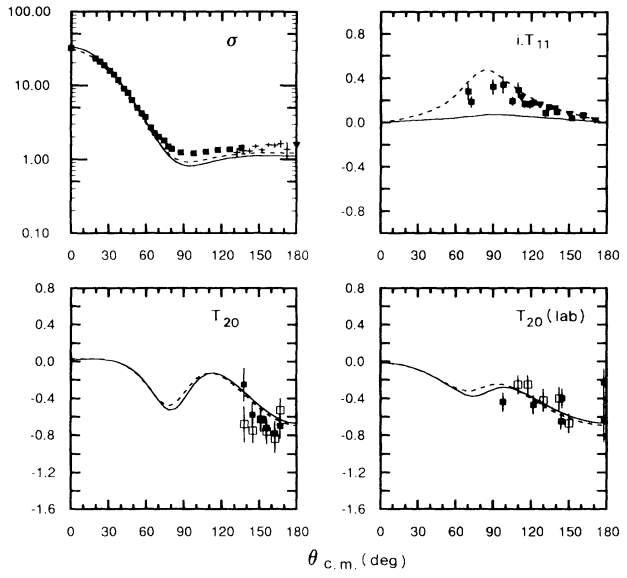

FIG. 5. πd elastic scattering observables at $T_\pi^{\rm lab} = 142$ MeV in the same conditions as in Fig. 4. The differential cross section (σ) is in mb/sr. Data are from the references cited in Refs. [6, 9].

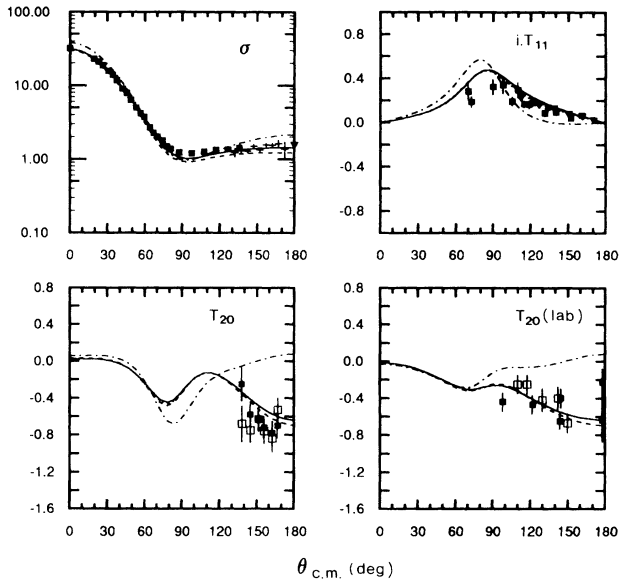

FIG. 6. πd elastic scattering observables at $T_\pi^{\rm lab} = 142$ MeV, calculated with the *modified* Tanabe-Ohta model (MTO), with different combinations of two-potential P_{11}–P_{33} models (A or B) and magic vectors [(a) or (b)]. The backward pion is introduced. Curves are (see notations in Table II): LY87 (dash-dotted line), MTO(b)-B (dashed line), MTO(a)-B (solid line), and MTO(a)-A (dotted line). At this energy, the dotted and solid curves are identical.

(MTO), and denoted as MTO(b)-B, where (b) stands for the definition of the magic vectors, and B refers to the P_{11}, P_{33} model (see Table II).

B. Comparison of the MTO and LY87 models

The MTO(b)-B model defined just above differs from the LY87 model in the following specific aspects: (1) description of the P_{11} and P_{33}, (2) backward-pion contribution versus off-shell modifications, and (3) *case-b* versus *case-a* magic vectors. The global effects on the πNN observables due to these differences are exhibited on Figs. 6–9 where we compare the MTO(b)-B (dashed line) and LY87 results (dash-dotted line). In Fig. 6, we show the πd elastic scattering observables $d\sigma/d\Omega$, iT_{11} and T_{20}, at $T_\pi^{\rm lab} = 142$ MeV. Clearly the MTO(b)-B model gives a much better description than LY87 for all the observables, especially for the tensor polarization T_{20}. This situation is also true at higher energies as shown in Fig. 7 at $T_\pi^{\rm lab} = 256$ MeV. We note that the experimental differential cross section is remarkably well reproduced by the MTO(b)-B model in the overall angular range. In particular, the cross section at backward angles at 256 MeV is considerably improved compared with the conventional three-body calculations which systematically overestimate this quantity. The differential cross section and asymmetry A_{y0} of the πd-NN reaction at $T_\pi^{\rm lab} = 142$ and 256 MeV are given in Fig. 8. The MTO(b)-B model gives the correct magnitude for $d\sigma/d\Omega$, but the wrong curvature, this defect becoming more pronounced as the energy increases. In comparison, the LY87 model does much better. Concerning the asymmetry A_{y0}, a mild structure is obtained with MTO(b)-B at 142 MeV, in line with the experimental data. This is

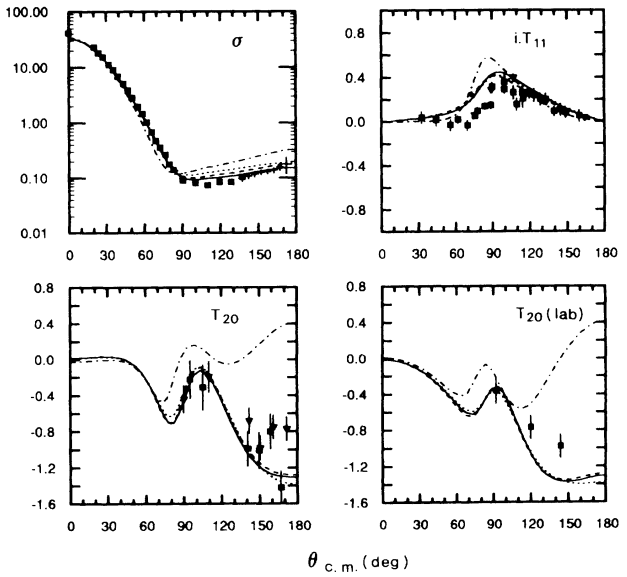

FIG. 7. πd elastic scattering observables at $T_\pi^{\rm lab} = 256$ MeV. Same legend as in Fig. 6.

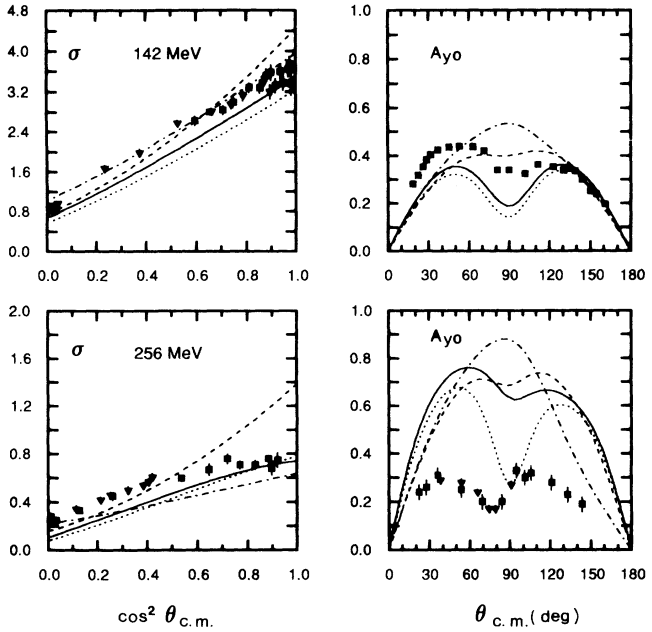

FIG. 8. πd-NN observables at $T_\pi^{\rm lab} = 142$ and 256 MeV. Same legend as in Fig. 6.

an encouraging result since this structure was impossible to obtain with LY87. This behavior persists at 256 MeV, but the magnitude becomes too large. The $^1D_2$ and $^3F_3$ NN phase parameters (real part δ and inelasticity ρ) are shown in Fig. 9. The characteristic of the MTO(b)-B model is to give contradictory repulsive effects in the $^1D_2$ and $^3F_3$ channels: the repulsion is too strong in $\delta(^1D_2)$, especially at high energy, while the lack of repulsion is obvious in $\delta(^3F_3)$. The situation is more favorable with the LY87 model, since the lack of repulsion which develops on both phase shifts at $T_N^{\rm lab} > 400$ MeV can be cured by heavy meson exchange contributions, as shown in Ref. [6]. That will not work in the MTO(b)-B model since $\delta(^1D_2)$ is already too repulsive. Concerning the inelasticity, the MTO(b)-B model does better than LY87 in both channels.

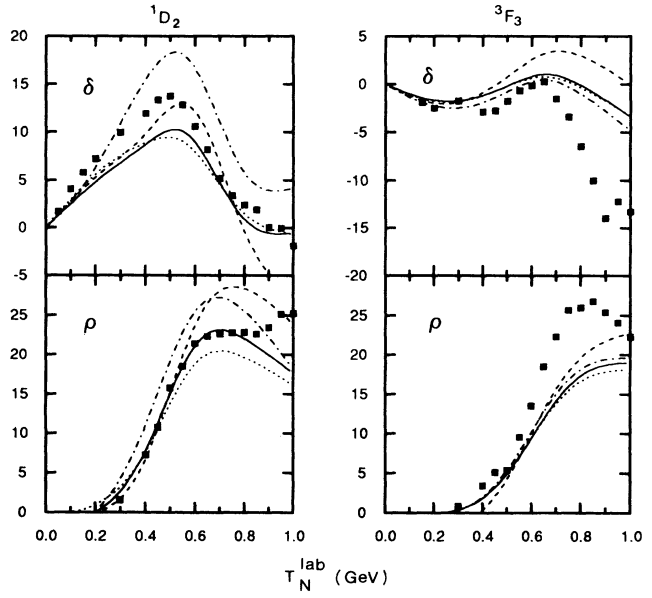

FIG. 9. $^1D_2$ and $^3F_3$ NN phase shift (δ) and inelasticity (ρ), in degrees. Same legend as in Fig. 6. Data are from Ref. [10].

In the remainder of this subsection, we analyze the origin of the most striking differences between the MTO(b)-B and LY87 models with respect to points (1)–(3) quoted above.

We first consider the tensor polarization T_{20} in πd elastic scattering. It is now well established that the T_{20} problem is closely related to the description of the P_{11} channel and to the implementation of the Pauli principle in the intermediate NN states. Here, we briefly recall the most important aspects in order to understand the present results. In the P_{11} model used in LY87, the repulsive contribution of the pole part is compensated by the attractive nonpole part to make the whole P_{11} amplitude weakly repulsive up to $T_\pi^{\rm lab} \sim 200$ MeV (corresponding to the small P_{11} phase shift observed at low energy). However, when this amplitude is used in the πNN equations, this cancellation does not exist in all three-body channels, since the Pauli principle excludes the intermediate NN channels coming from the pole part. For such Pauli forbidden states, only the nonpole part contributes. The consequence is that the predicted T_{20} is systematically higher than the data at backward angles (see Figs. 6 and 7 above, dash-dotted line), while a pure three-body model without the P_{11} input reproduces the data rather well (see Figs. 8–10 in Ref. [9]). This situation is common to all three-body models using the explicit decomposition of the P_{11} amplitude into a pole and nonpole part. Recently, we have shown how it is possible to improve this situation, not only for T_{20} but also for the other πd observables, by introducing the so-called Jennings mechanism; see Ref. [9] for all the details. In the MTO(b)-B model, the P_{11} is treated as a single entity, as explained before, and the Pauli principle is applied "globally" to the corresponding three-body channels. This turns out to be practically the same as if the P_{11} input is not included. For this reason, the MTO(b)-B results are in good agreement with the data, especially T_{20} (see Figs. 6 and 7, dashed line). We note that such a cancellation effect was demonstrated previously by Afnan and MacLeod [17]: starting from a three-body model with the P_{11} amplitude divided into pole and nonpole parts, they found that T_{20} is correctly described only when the nonpole contribution is not included in the Pauli forbidden channels (see Figs. 8 and 9 in Ref. [17]).

Second, we discuss the effect of the backward propagating pion. As pointed out by Tanabe and Ohta in Ref. [11], this contribution is indispensable in obtaining the correct magnitude of the πd-NN cross section. Indeed, a factor of ~ 2 is missing when this contribution is not taken into account in the MTO(b)-B calculation. How-

ever, the backward pion is not the whole story as we now explain. In the LY87 approach, the πd-NN cross section is underestimated by a factor of ~ 4 when the (one-term) Δ-isobar model is used in the P_{33} channel. As mentioned in the Introduction, this is due to the too soft form factor used in that channel, and this situation was cured by introducing off-shell modifications. As a test we have added the backward pion contribution to the LY87 model and at the same time discarded the off-shell modification from it. The resulting πd-NN cross section is found to be still underestimated by a factor of ~ 2, indicating that the backward pion contribution compensates only partially the effects due to the inappropriate off-shell behavior of the P_{33} channel. As shown by TO [11] and as we will see later, this situation can be improved by using a two-term P_{33}. We may therefore conclude that the right magnitude of the πd-NN cross section results from the *combined* effects of the backward pion contribution and of the two-potential model used in the P_{33} channel.

We now examine the sensitivity of the πNN observables to the choice *case-a* or *case-b* magic vectors. As observed by Tanabe and Ohta in Ref. [11], those two choices induce sizable differences in the ${}^1D_2$ and ${}^3F_3$ NN phase parameters. Such differences should also appear in the πd-NN sector, as the ${}^1D_2$ channel has an important contribution to the cross section. However, Tanabe and Ohta did not investigate this point in Ref. [11] where only *case b* was retained. In the MTO(b)-B calculations presented in Figs. 6–9 above (dashed curves), *case b* was also chosen. We now present in the same figures the results obtained with the *case-a* magic vectors [MTO(a)-B model, solid line curves]. The sensitivity of the NN phase parameters to the two choices develops above $T_N^{\rm lab} \sim 400$ MeV (Fig. 9). In comparison with the experimental data, the *case-a* ${}^1D_2$ phase shift exhibits a better behavior than *case b* at energies above 600 MeV, but is too repulsive in the region of the maximum. The ${}^1D_2$ inelasticity is very well reproduced with *case a* up to 700 MeV, but the tendency at higher energy disagrees with the data. In the ${}^3F_3$ channel, *case a* does better than *case b* for the phase shift (which remains too attractive above 700 MeV), but not for the inelasticity which becomes even smaller above 600 MeV. In the πd-NN sector, the curvature of the differential cross section which was wrong with MTO(b)-B, is considerably improved with MTO(a)-B, the improvement becoming even more spectacular as the energy increases (Fig. 8). However, the magnitude is slightly underestimated at all energies. We note that these results are now in line with those of the LY87 model (dash-dotted line) where *case-a* magic vectors are also used. Concerning the asymmetry A_{y0}, a somewhat more pronounced structure is obtained with *case a*, in line with the experimental data at $T_\pi^{\rm lab} = 142$ MeV, but the magnitude still remains too large at 256 MeV (Fig. 8). Finally, the πd elastic scattering observables are quite insensitive to the choice of the magic vectors, the MTO(a),(b)-B curves being practically identical (see Figs. 6 and 7). From these results, it appears that in the MTO model, *case-a* magic vectors must be preferred to *case-b*. For these reasons, we will use the *case-a* choice in the following (this choice was also retained *a priori* in our LY87 calculations from a purely numerical point of view, as explained in Sec. II E).

Finally, we have examined to what extent the πNN observables are modified when model A is used for the P_{11} and P_{33} channels in the MTO(a) model. As can be seen in Figs. 6–9, the differences between MTO(a)-A (dotted curves) and MTO(a)-B (solid curves) are small. The largest difference appears in the asymmetry A_{y0} of the πd-NN reaction at 256 MeV which takes a very pronounced structure with model A (we note that similar effects were observed by Tanabe and Ohta; see Fig. 3 in Ref. [12]). From examination of Figs. 6-9, it appears that model B is a little better choice. Recall, however, the large Δ mass renormalization characterizing this model (see Sec. II A).

In closing this subsection, we may conclude that the MTO model (using *case-a* magic vectors) is able to give a reasonable overall description of the πNN observables at medium energies. The main advantage over the LY87 approach is that the physics of the problem is better described through the use of a two-potential model for the P_{33} combined with the backward propagating pion contribution. However, it should be kept in mind that even if the πd elastic scattering observables are quite reasonably reproduced, the two-potential model of the P_{11} channel as used in the manner of TO is not satisfactory in view of its violation of the Pauli principle. Also this approach has resulted in a too repulsive ${}^1D_2$ phase shift, which would become even more repulsive upon inclusion of the heavy meson exchanges (note that within the TO treatment of the P_{11} channel as stated above, how to include heavy meson exchange effects is not very clearly defined while respecting the Pauli principle).

C. Mixed model

It now seems reasonable to expect that a *mixed* version, combining the desirable aspects of the Tanabe-Ohta and LY87 models, should produce a better model. It is clear that (i) from the TO approach we must retain the two-potential model for the P_{33} and the backward pion contribution, which in combination give a correct off-shell behavior in the $\pi d - NN$ reaction, and (ii) from the LY87 approach we must take the P_{11} model with the explicit separation into pole and nonpole parts, thus guaranteeing the correct treatment of the Pauli principle in the three-body equations. So, we define a *mixed* model (hereafter referred to as LYTO) as the upgraded MTO(a) model (recall the last subsection) where the P_{11} of the LY87 approach is now used. This is equivalent to modifying the LY87 model by adopting a two-potential model for the P_{33}, together with introducing the backward pion and discarding the off-shell modifications. To be definite, the LYTO model uses *case-a* magic vectors and contains the backward pion contribution (in $Z_{N\Delta}$, $Z_{\Delta N}$, and $Z_{\Delta\Delta}$), and is equipped with the following two-body input: the d-NN, all small πN and P_{11} are from LY87, and two-term P_{33} potentials are from TO (models

A, B) or of the Saxon form discussed earlier in Sec. II A (see Table II).

We have first studied briefly how the difference in the P_{33} model is reflected in the πNN channels. Then it has turned out that the TO model A and Saxon give quite similar results in all the channels. As already discussed in Sec. II A (Fig. 1), the behaviors of the half-off-shell functions corresponding to these models are different only for off-shell momentum greater than 600 MeV/c, where the off-shell variation is apparently not essential for the πNN observables. So we present in Figs. 10–12, 15–16 only the results with model B (dashed line) and Saxon P_{33} (solid line).

(i) πd *elastic scattering.* A complete set of results including the differential cross section, and the vector and tensor polarizations calculated at $T_\pi^{\rm lab} = 142$, 180, and 256 MeV are shown in Figs. 10–12. The results with model-B and Saxon parametrizations are close, which are then similar to the LY87 results in Figs. 6 and 7 above (dash-dotted curves), with a little preference to be given to the Saxon P_{33}. In particular, we find, as anticipated, (a) too high differential cross sections at large angles for 256 MeV, (b) not especially good result in the it_{11}, and (c) the trouble with T_{20} at backward angles which characterizes the calculations with the explicit pole and nonpole decomposition of the P_{11}, as discussed earlier. From Ref. [9], one might then well expect that this can be cured by introducing the terms corresponding to the Jennings mechanism. However, unlike with the LY87 πd amplitudes used in Ref. [9], the Jennings mechanism has been found not to really give improvement in T_{20} and it_{11} when combined with the present LYTO amplitudes. A typical result at 256 MeV is presented in Fig. 12 (dotted line). This was quite disturbing in view of our detailed study of the Jennings mechanism in a covariant formalism [9]. So we have compared the LY87 and LYTO πd partial wave amplitudes. Then it has turned out that the major difference between those sets of amplitudes, which brings about different predictions in those two observables upon including the Jennings term, may be localized to the 0^+ and 1^+ partial waves. Furthermore, we have found that it is the combination of the backward pion contribution and the difference in the off-shell structure of the P_{33} amplitudes that does make the difference in those partial waves. This then indicates that even with the same P_{11} input these particular partial waves are sensitive to how

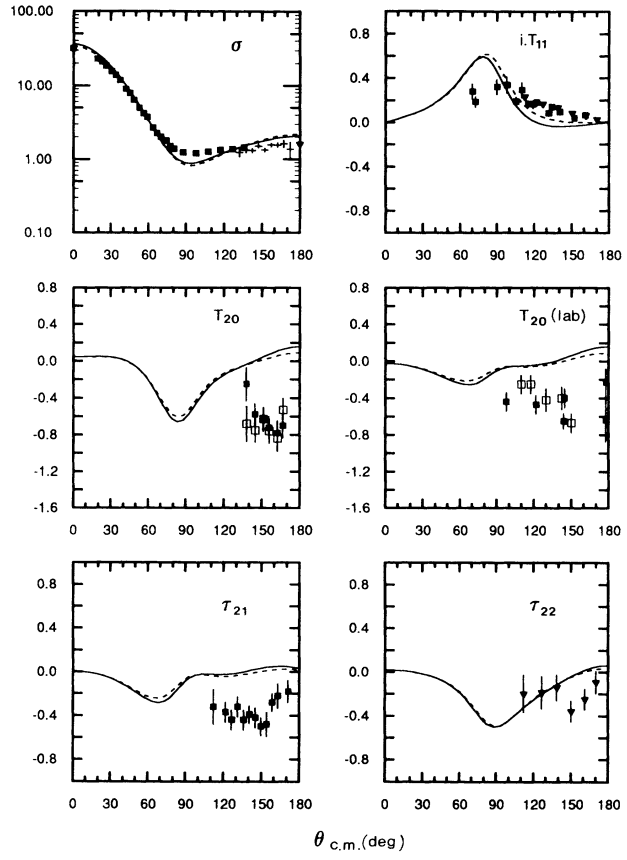

FIG. 10. πd elastic scattering observables at $T_\pi^{\rm lab} = 142$ MeV, calculated with the *mixed* Tanabe-Ohta/LY87 model (LYTO, see Table II), with different two-potential P_{33} models. The backward pion is introduced, and *case-a* magic vectors are used. Curves are P_{33} Saxon (solid line) and P_{33} model B (dashed line).

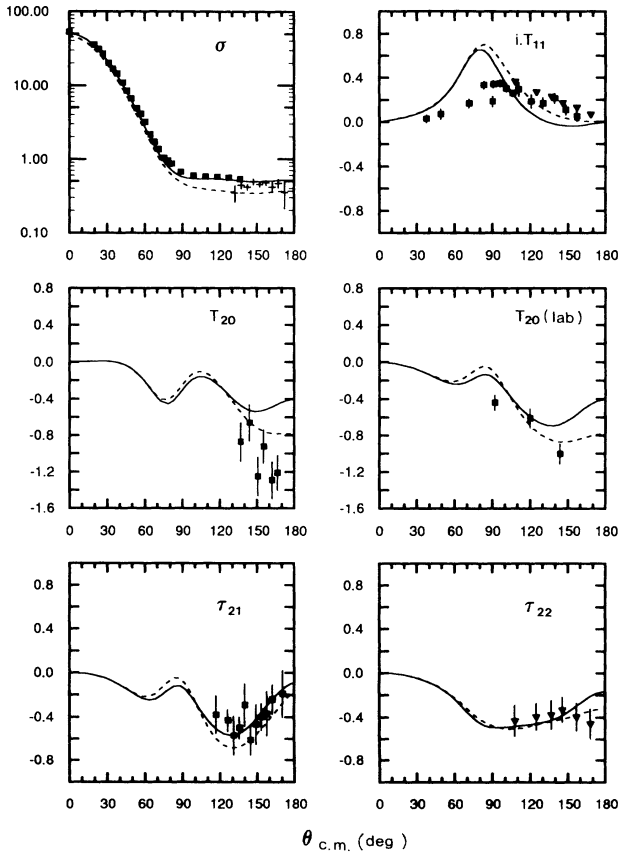

FIG. 11. πd elastic scattering observables at $T_\pi^{\rm lab} = 180$ MeV. Same legend as in Fig. 10.

the pion exchange and the degree to which the off-shell P_{33} amplitude are treated in a given model: the sensitivity brought in predominantly by the process depicted in Fig. 13. Clearly, this does not sound reasonable: this apparent sensitivity must be compensated by something. We then argue that the Jennings mechanism, as its simplest form suggested in Ref. [25] and investigated in Ref. [9], should be extended to include at least the contribution shown in Fig. 14, which should serve to solve this problem. This may be inferred from how the original Jennings term was introduced [25]. We want to remark here that this contribution was suggested in Ref. [9] from a somewhat different context: to give a plausible energy dependence to the Jennings mechanism. The actual cal-

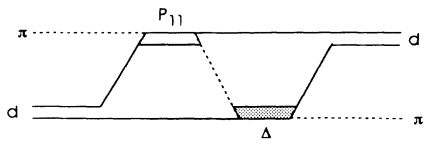

FIG. 13. Graph which sensitively influences the 0^+ and 1^+ elastic πd partial waves, regarding the backward pion contribution and the off-shell structure at the P_{33} vertices.

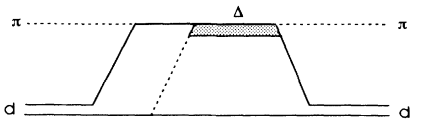

FIG. 14. The lowest order correction to the original Jennings mechanism.

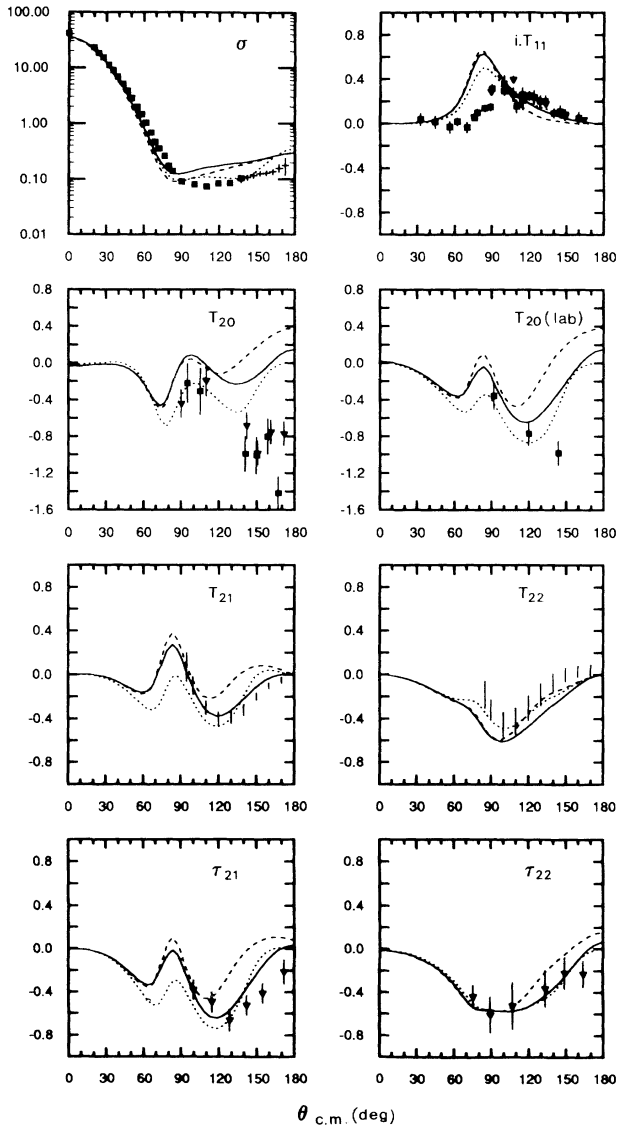

FIG. 12. πd elastic scattering observables at $T_\pi^{\rm lab} = 256$ MeV. Same legend as in Fig. 10. The dotted curve is the calculation with P_{33} Saxon including the Jennings term.

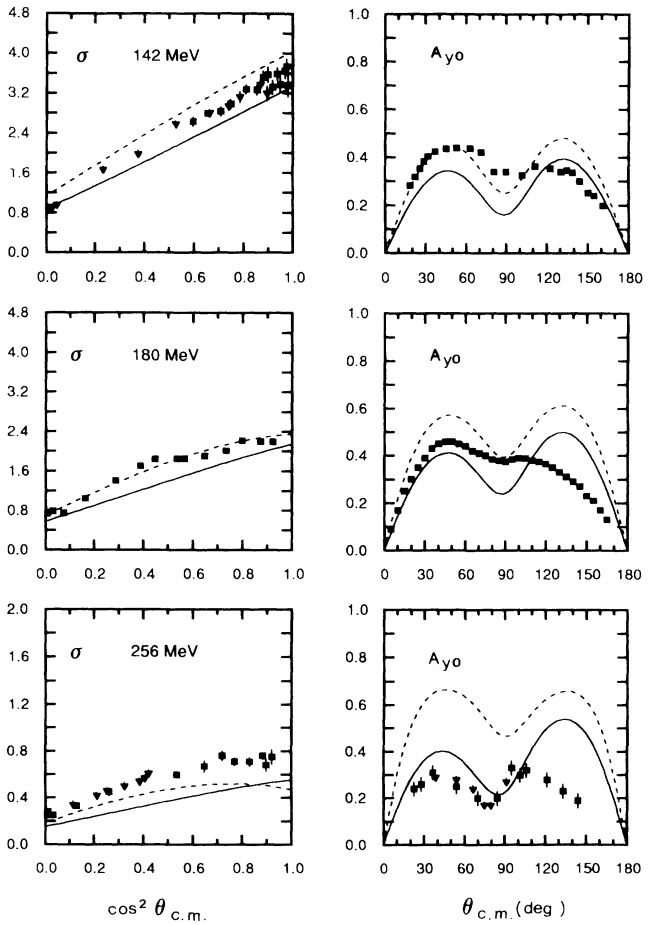

FIG. 15. πd-NN observables at $T_\pi^{\rm lab} = 142$, 180, and 256 MeV. Same legend as in Fig. 10.

culation of this contribution is quite difficult, however.

(ii) *πd-NN reaction.* The differential cross section and asymmetry A_{y0} at $T_\pi^{\rm lab} = 142$, 180, and 256 MeV are given in Fig. 15. At 142 MeV, the Saxon P_{33} does better than model B which overestimates the cross section in comparison with the data, but the situation reverses at higher energy. Comparing with the dash-dotted curves in Fig. 8, we see that the LYTO cross sections are lower than the LY87 results. However, the agreement with the experimental data remains satisfactory, especially in view of the curvature which is correctly reproduced. The prominent result is that the asymmetry A_{y0} is quite reasonably described by the model-B and Saxon calculations, in both its structure and the magnitude (model-B result is somewhat too high at 256 MeV though). In this channel it is not easy to tell which of the two P_{33} models is more favorable, but at least both fare better than the LY87 model globally.

(iii) *NN elastic scattering.* The $^1D_2$ and $^3F_3$ phase parameters are shown in Fig. 16. Compared with the LY87 results in Fig. 9, both model B and Saxon give more repulsive $^1D_2$ and less repulsive $^3F_3$, with comparable or better description of the inelasticity parameter in both channels. The lack of repulsion which manifests on both phase shifts at high energy is compensated by introducing the contribution of heavy meson exchange effects, according to the method described in Ref. [6]. The results in the Saxon case are shown in Fig. 16 (dotted line). Model-B result has a problem in this respect: with the introduction of heavy mesons the $^1D_2$ phase above $T_N^{\rm lab}$ $\sim$ 600 MeV will certainly become lower than the data. The inelasticities are practically unchanged by the heavy mesons (especially in $^3F_3$), as it was the case in the LY87 calculations. Note also that these contributions do not bring any significant change in the πd elastic and πd-NN observables. Globally, within the two-term P_{33} interactions we have investigated, Saxon model fares better than model B in this channel, but, like all the existing models, neither of them can escape the lack of inelasticity in the $^3F_3$ partial wave.

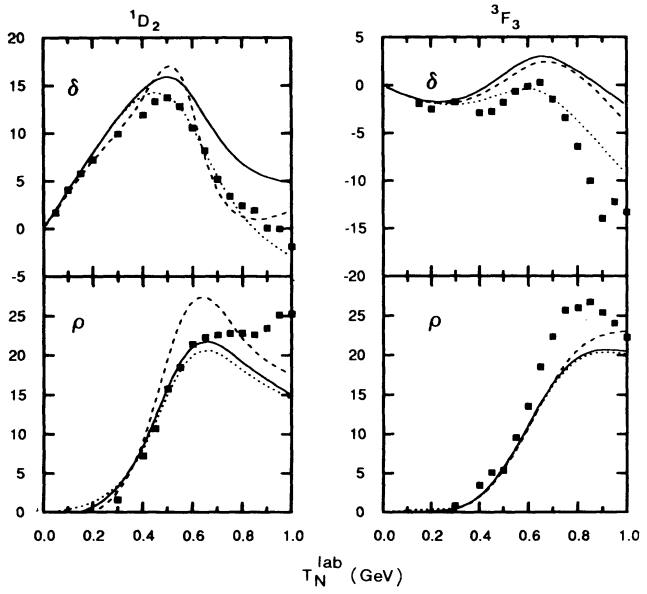

FIG. 16. $^1D_2$ and $^3F_3$ NN phase parameters. Same legend as in Fig. 10. The dotted curves are the Saxon results with the contribution of the heavy meson exchange effects.

IV. CONCLUSION

Our principal effort in this article has been the two-term P_{33} interaction originally proposed by Tanabe and Ohta in the context of various πNN observables. One of the main reasons to prefer this type of interaction to the usual one-term isobar model is that the former is more consistent with quark models, thus a little less phenomenological. For example, the static quark model prediction of the $\pi N\Delta$ coupling constant is $f^2_{\pi N\Delta}/4\pi \sim 0.24$ while the corresponding quantity extracted from model A, model B, and Saxon turn out to be 0.24, 0.21, and 0.26, respectively. These are to be compared with the one from the one-term isobar result of 0.35. Another reason is that when used in the πNN system the one-term P_{33} isobar interaction must be supplemented by an *ad hoc* off-shell modification, to be consistent with the data.

The Tanabe-Ohta (TO) approach is the first πNN model with two-term P_{33} interactions, and within this approach we have investigated such effects as the backward propagating pion, choice of magic vectors, difference due to different P_{33} interactions, etc. As compared with the one-term isobar model used in LY87, the modified Tanabe-Ohta approach (MTO) gives a more reasonable account of the πd-NN observables, in particular of the asymmetry A_{y0}. The curvature of the differential cross section is correctly reproduced only with the *case-a* magic vector. So we prefer it. This could be due to the fact that strictly speaking our contour rotation method is only compatible with this choice. Other integration methods as adopted, for example, in Ref. [8] might consistently accomodate the choice of *case-b* magic vectors. As for the elastic NN channel one finds that there are problems: (1) excessive repulsion in the $\delta(^1D_2)$ already before including the effect of heavy meson exchanges, and (2) the lack of inelasticity in the $^3F_3$. We have then completed the TO calculations by studying the elastic πd channel. The result in this channel has turned out to be quite good: the differential cross section at $T_\pi^{\rm lab} =$ 256 MeV may be considered the best of all the existing models. There is a problem, however, that this result is based upon the treatment of the πN P_{11} input in the TO approach where the Pauli principle is not respected in the NN states.

Then we have devised the *mixed model* (LYTO) in an attempt to improve the TO approach. With the correct implementation of the Pauli principle inherent in this model, predictions of some of the πd observables like the large angle T_{20} become worse than in the TO model, just like in the LY87 result. Upon analyzing this situation, we have observed that the Jennings term, which has been accepted as curing the T_{20} problem, must include the next order correction, as anticipated in Ref. [9]. The result in the πd-NN channel has turned out to be compa-

rable or somewhat better than the TO model, and in the elastic NN channel, the predictions are preferable to the TO result, the $^1D_2$ phase shift, in particular, with due consideration of the heavy meson exchanges. Conservatively speaking, the overall quality of the prediction by this model has been found to be about the same as that by the LY87 model, but with a remarkable improvement in the πd-NN asymmetry A_{y0}. Thus we believe that a *mixed model* type approach investigated here should be considered as the basis for future studies in the πNN system. As a first step we have recently studied the process $NN \to N\Delta$ in the context of this mixed model, which will be reported elsewhere [26]. Of course within this approach one still needs to investigate improvements in the P_{33} and P_{11} interactions in order to attack the persistent problem of the insufficient inelastic strength in the $^3F_3$ channel (or more generally *the spin triplet problem*).

ACKNOWLEDGMENTS

One of us (T.M.) would like to thank A. C. Fonseca for warm hospitality extended to him at Centro de Fisica Nuclear da Universidade de Lisboa, Portugal. He is also grateful to CEN Saclay and IPN Lyon, France, for offering him a few visits in the course of this work. Another (C.F.) is thankful to the Physics Department, VPI & SU for kind hospitality during his visit there. A partial support by the U.S. Department of Energy under Grant No. DE-FG-ER40413 is greatly appreciated.

[1] H. Garcilazo and T. Mizutani, *πNN Systems* (World Scientific, Singapore, 1990).
[2] I. R. Afnan and A. W. Thomas, Phys. Rev. C **10**, 109 (1974).
[3] Y. Avishai and T. Mizutani, Nucl. Phys. **A326**, 352 (1979); **A338**, 377 (1980).
[4] I. R. Afnan and B. Blankleider, Phys. Lett. **93B**, 367 (1980); Phys. Rev. C **22**, 1638 (1980); B. Blankleider and I. R. Afnan, *ibid.* **24**, 1572 (1981).
[5] A. S. Rinat, E. Hammel, Y. Starkand, and A. W. Thomas, Nucl. Phys. **A329**, 285 (1979); A. S. Rinat, Y. Starkand, and E. Hammel, *ibid.* **A364**, 486 (1981); A. S. Rinat and Y. Starkand, *ibid.* **A397**, 381 (1983).
[6] G.-H. Lamot, J. L. Perrot, C. Fayard, and T. Mizutani, Phys. Rev. C **35**, 239 (1987).
[7] T.-S. H. Lee and A. Matsuyama, Phys. Rev. C **36**, 1439 (1987); A. Matsuyama and T.-S. H. Lee, Nucl. Phys. **A256**, 547 (1991).
[8] H. Garcilazo, Phys. Rev. C **35**, 1804 (1987).
[9] T. Mizutani, C. Fayard, G.-H. Lamot, and B. Saghai, Phys. Rev. C **40**, 2763 (1989).
[10] R. A. Arndt, J. S. Hyslop III, and L. D. Roper, Phys. Rev. D **35**, 128 (1987).
[11] H. Tanabe and K. Ohta, Nucl. Phys. **A484**, 493 (1988).
[12] H. Tanabe and K. Ohta, Phys. Rev. C **36**, 2495 (1987).
[13] T. Mizutani, C. Fayard, G.-H. Lamot, and R. S. Nahabetian, Phys. Rev. C **24**, 2633 (1981).
[14] T. Mizutani, B. Saghai, C. Fayard, and G.-H. Lamot, Phys. Rev. C **35**, 667 (1987).
[15] S. Nozawa, B. Blankleider, and T.-S. H. Lee, Nucl. Phys. **A513**, 459 (1990).
[16] B. J. VerWest, Phys. Lett. **83B**, 161 (1979).
[17] I. R. Afnan and R. J. MacLeod, Phys. Rev. C **31**, 1821 (1985).
[18] G.-H. Lamot, C. Fayard, T. Mizutani, and B. Saghai, Contribution to Few Body XI Conference, Tokyo/Sendai, Supplement to Research Report of Laboratory of Nuclear Science, Tohoku University, 1986, Vol. 19, p. 32.
[19] K. Schwarz, H. F. K. Zingl, and L. Mattelitsch, Phys. Lett. **83B**, 297 (1979).
[20] J. Haidenbauer and W. Plessas, Phys. Rev. C **30**, 1822 (1984).
[21] R. Aaron, R. D. Amado, and J. E. Young, Phys. Rev. **174**, 2022 (1968).
[22] A. S. Rinat and A. W. Thomas, Nucl. Phys. **A282**, 365 (1977).
[23] T. Ueda, Nucl. Phys. **A463**, 69c (1987).
[24] W. M. Kloet and R. R. Silbar, Nucl. Phys. **A338**, 281 (1980).
[25] B. K. Jennings, Phys. Lett. B **205**, 187 (1988).
[26] C. Fayard, G.-H. Lamot, T. Mizutani, and B. Saghai (in preparation).

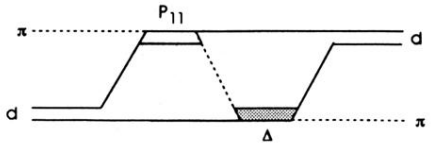

FIG. 13. Graph which sensitively influences the 0^+ and 1^+ elastic πd partial waves, regarding the backward pion contribution and the off-shell structure at the P_{33} vertices.

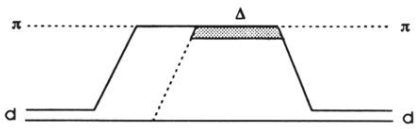

FIG. 14. The lowest order correction to the original Jennings mechanism.